Tutor/s

Dr. Fèlix Urpí Tubella
Departament de Química Inorgànica i Orgànica

Dr. José Luís Abad Saiz
RUBAM-IQAC-CSIC

Grau de Química

Treball Final de Grau

Synthesis of DES1 inhibitors to study the sphingolipid metabolism in non-alcoholic fatty liver disease.

Síntesi d'inhibidors de DES1 per a l'estudi del metabolisme d'esfingolípids a la malaltia del fetge gras no alcohòlic.

Cristina Bello Quiñones

June 2022

UNIVERSITAT DE BARCELONA

B:KC Barcelona Knowledge Campus
Campus d'Excel·lència Internacional

M’agradaria donar les gràcies al Dr. José Luis Abad per obrir-me les portes del seu laboratori i ajudar-me en el transcurs del meu projecte i aprenentatge. Així com també als meus amics i família pel seu suport incondicional sobretot durant aquests últims mesos.

REPORT

IDENTIFICATION AND REFLECTION ON THE SUSTAINABLE DEVELOPMENT GOALS (ODS)

Global health is one of the main concerns of the actual society. The COVID-19 crisis has demonstrated how important and essential it is to provide population with quality and public health, as well as being prepared for such a sanitary emergency. Regarding health improvement, research investment is one focal point since it is the only way of developing new or better treatments and cures.

This project suits in the third sustainable development goal (people area), named good health and well-being, which states that ensuring a healthy life and promoting the population's well-being is an essential point of worldwide sustainable development.

The reason lies in the aim of this work, which is the development of potential therapeutic agents for non-alcoholic fatty liver disease (NAFLD). The mentioned disease has a 15-25% of prevalence in global population. Therefore, the project utterly adjusts to goal 3; more concretely it can be included in target 3.4, which intends to decrease the premature mortality due to not communicable diseases through prevention and treatment. Although further research must be done, this path definitively has the potential to improve NAFLD prevention.

CONTENTS

1. SUMMARY

Evidence indicates that ceramides, and more recently dihydroceramides, are involved in several biological processes, such as sphingolipid metabolism and cell signalling. Furthermore, it is believed that they have critical roles in insulin resistance, oxidative stress and inflammation, which are pathologies associated with non-alcoholic fatty liver disease (NAFLD). Therefore, these bioactive molecules and the enzyme that regulates the conversion of ceramide into dihydroceramide (DES1) are potential therapeutic targets [1][2][3].

This project has successfully prepared two compounds for the study of their potential inhibition activity over DES1. They consisted in the preparation at larger scale of a potential therapeutic drug (*N*-(4-hydroxyphenyl)garcinamide, **2**) to treat mice fed with a high-fat diet and a new class of inhibitors for hepatic cell cultures ((*E*)-Δ^6 ceramides), for which a new synthetic route was developed. Concretely, the synthesized inhibitor of this class was *N*-((2*S*,3*R*,*E*)-1,3-dihydroxyoctadec-6-en-2-yl)pivaloylamide (**8**). These compounds were characterized by NMR and mass spectroscopy analysis.

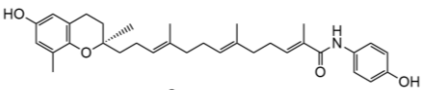

2

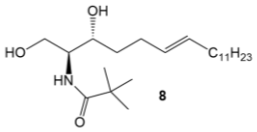

8

Keywords: NAFLD, sphingolipid, DES1, inhibitors, ceramide, dihydroceramide, garcinoic acid, diastereoselective reduction.

2. RESUM

Múltiples estudis indiquen que les ceramides, i més recentment les dihidroceramides, estan involucrades en diversos processos biològics, com ara el metabolisme dels esfingolípids i la senyalització cel·lular. A més, es creu que tenen un paper crític en el desenvolupament de la resistència a la insulina, l'estrès oxidatiu i la inflamació, les quals són patologies associades a la malaltia del fetge gras no alcohòlic (MFGNA). Per tant, aquestes molècules bioactives i l'enzim que regula la conversió de ceramida en dihidroceramida (DES1) són potencials objectius terapèutics [1][2][3].

En aquest projecte s'ha preparat amb èxit dos compostos per a l'estudi de la seva potencial activitat d'inhibició sobre la DES1. Aquests van consistir en la preparació a major escala d'un potencial fàrmac terapèutic (*N*-(4-hidroxifenil)garcinamida, **2**) per tractar ratolins alimentats amb una dieta alta en greixos i una nova classe d'inhibidors per als cultius cel·lulars hepàtics ((*E*)-Δ^6 ceramides), per a aquest últim es va desenvolupar una nova ruta sintètica. Concretament, l'inhibidor sintetitzat d'aquesta classe va ser *N*-(2*S*,3*R*,*E*)-1,3-dihidroxictadec-6-en-2-yl)pivaloylamida (**8**). Aquests compostos es van caracteritzar per l'anàlisi de RMN i espectroscòpia de masses.

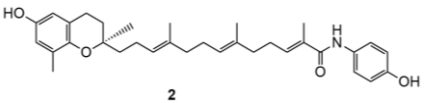

2

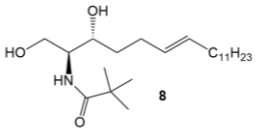

8

Paraules clau: MFGNA, esfingolípid, DES1, inhibidors, ceramida, dihidroceramida, àcid garcinoic, reducció diastereoselectiva.

3. INTRODUCTION

Non-alcoholic fatty liver disease (NAFLD) is a liver illness that has a great impact in worldwide health since it is a chronic and progressive disorder. Its development involves different stages. The very first one is hepatic steatosis, which have a huge prevalence in global population (15-25%) [1], making it one of the most common chronic diseases in the developed countries. Despite being reversible, steatosis can lead to more critical stages such as non-alcoholic steatohepatitis (NASH), estimated to be present in 5-17% of the population, cirrhosis, and hepatocellular carcinoma [2]. The development of steatosis can be described as an accumulation of triacylglycerols (TAGs) caused by an increase in the calorie intake and *de novo* lipogenesis. However, there is evidence that sphingolipids (SLs), and more concrete ceramides (Cer), have a decisive role in NAFLD and its severe complications.

3.1. SPHINGOLIPID METABOLISM

Sphingolipids are a class of bioactive molecules that play essential roles in the metabolism of most living beings. They are consisted of a sphingoid base (sphingosine/sphinganine) backbone which can be attached to a fatty acid through an amide bond and can be substituted at the primary hydroxyl carbon. Thus, depending on which is this mentioned substituent, SLs can be divided into four subfamilies: phosphosphingolipid, glycosphingolipids, sphingoid bases and ceramides. The most relevant structure is Cer, containing just a hydrogen as a substituent at the primary alcohol (Fig. 1). Glycosphingolipids and phosphosphingolipids have though more complex structures. These compounds bear a sugar or a phosphocholine, respectively.

SLs not only can function as a structural component of membranes, as it has always been known, but they also have important functions in cell signalling, secretion and endocytosis.

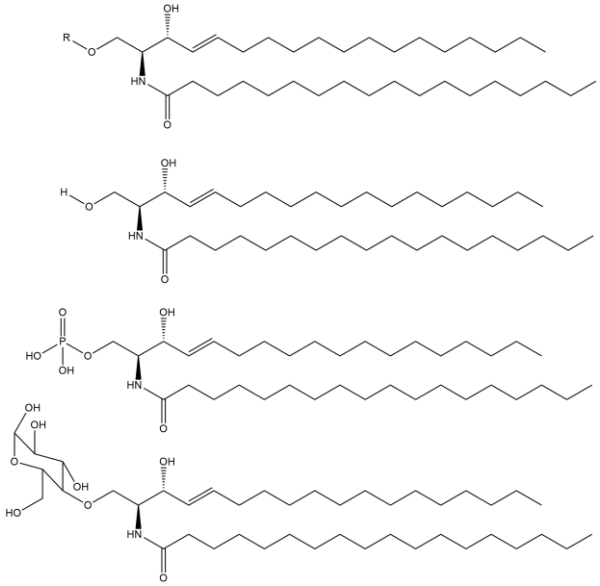

Figure 1.- General structure of SLs and different SLs subfamilies

3.1.1. Ceramide synthesis

Cers are a focal point of the SLs metabolism since their biosynthesis is carried out in the intersection of different anabolic and catabolic pathways. They can be synthesized by three different alternatives.

The first one and the main contributor to Cers production is *de novo* biosynthesis, which takes place in the ER. This path starts with the condensation of serine and palmitoyl-CoA to form sphinganine by action of the serine palmitoyltransferase (SPT). The second step consists in the production of dihydroceramide (dhCer) thanks to the acylation undertaken by the ceramide synthase (CerS). At this point, DES1 (Δ-4-dihydroceramide desaturase 1) desaturates dhCer giving rise the corresponding Cer (Fig. 2) [1].

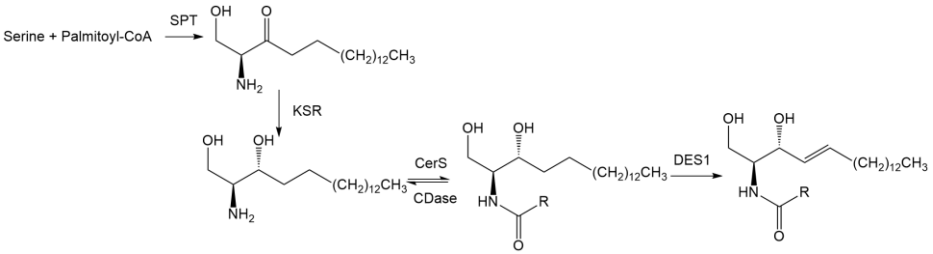

Figure 2.- Ceramide synthesis through *de novo* pathway

Once Cer has been formed, it can be exported to the Golgi apparatus through vesicular transport or CERT to be transformed into sphingomyelin or glucosylceramide. Both of these are carried to the plasma membrane, where sphingomyelin can convert into ceramide due to the action of sphingomyelinases (SMase), being the second pathway of ceramide synthesis [1].

In the plasma membrane, ceramide be turned into sphingosine, another bioactive molecule that can be incorporated in the ER to be transformed back into ceramide through the salvage pathway [1].

3.1.2. Role of ceramides in NAFLD

As mentioned before, the function of Cers is not limited to being the integral structure of the cell membrane's lipid bilayer, yet they have several roles in cell-signalling. Furthermore, their accumulation in the liver due to an increase of free fatty acids (FFA), such as palmitic acid, influx may contribute to insulin resistance and oxidative stress [2]. Thus, it is thought that Cers have an inhibitor role in insulin signalling and they induce oxidative stress and inflammation, all of which are related to NAFLD, presenting the possibility of Cers being biomarkers in both NAFLD and NASH.

3.1.2.1. Role of ceramides in lipid-induced insulin resistance

NAFLD is highly correlated with insulin resistance and Cers are bioactive molecules that relate to several pathways implicated in this condition, such as inflammation, oxidative stress and apoptosis.

Insulin signalling consists of several correlated processes that lead to glucose uptake and glycogen synthesis and storage [1]. There are four different pathways through which Cer can regulate this cascade of events.

First, Cer can activate and stimulate both PKCζ and phosphatase 2A (PP2A), enzymes which phosphorylates one of the domains of Akt/PKB, an important intermediate in insulin signalling, leading to the blocking of its translocation from the cytoplasm to the plasma membrane and, therefore, its activation (Fig. 3) [1].

A second pathway may be the alteration of the plasma membrane fluidity by action of Cer. This leads to the disturbance in the fusion of GLUT4 into the plasma and, consequently, directly blocking glucose entrance.

Another alternative is the activation of PKR, which phosphorylates IRS1 (insulin reception substrate) preventing its activation and therefore modifying the hepatic insulin signalling.

In a similar way, IRS1 can be inhibited by action of ceramide through NLRP3 inflammasome pathway.

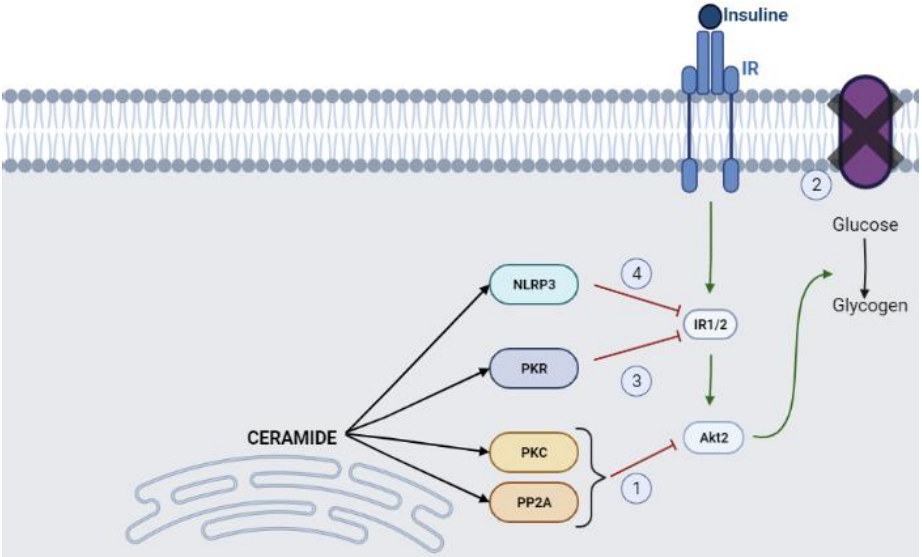

Figure 3.- Role of ceramides in lipid-induced insulin resistance

Cer is not the only one sphingolipid related to insulin regulation. Other SLs are involved in such functions. For example, sphingosine-1-phosphate (S1P) has proven to impair insulin signalling in hepatocytes and leads to nutrient intake. Thus, Cer and S1P have opposing effects in this topic [1].

3.1.2.2. Ceramides and cytokine-mediated hepatic inflammation

TNF-α are proinflammatories cytokines that can activate SMase and, consequently, increase Cer synthesis. Apart from inducing insulin resistance, the interaction between TNF-α and Cers can lead to an increase in mitochondrial generation of reactive oxygen species, fact that promotes apoptosis and additional accumulation of inflammatory cells in the liver, causing an aggravation of hepatic inflammation [2].

However, it has been observed that there is an anti-inflammatory cytokine, adiponectin, which can decrease Cer levels by upregulating ceramidase (CDase) and, therefore, stimulating the conversion of Cer into S1P [2]. Hence, it can be said that adiponectin improves insulin sensitivity by decreasing Cer levels and promoting S1P formation. Besides it can supress lipogenesis and enhance oxidation of FFAs in the mitochondria, decreasing then hepatic lipid accumulation.

These facts strongly demonstrate the linkage between inflammation and insulin resistance, since it can be regulated by action of cytokines.

Taking into consideration all this evidence, a model of Cers in the development and progression of NAFLD can be proposed. In this model, it can be said that obesity-induced insulin resistance result in an increase in proinflammatory cytokines (TNF-α) production and FFA discharge, and a decrease in adiponectin levels. All these intermediaries gather in the liver, where Cer production is stimulated by them, thus promoting hepatic insulin resistance, through the paths previously detailed, and apoptosis. The role of adiponectin in Cer levels lies in its action over CDase, promoting conversion of Cer into S1P [2].

Hence, although further work is required to fully understand the role of Cers, evidence show the implication of SLs in pathologies associated with NAFLD.

3.1.3. Dihydroceramide as a key metabolite

It has always been thought that dihydroceramides were just an inert metabolite whose only role was being an intermediate in the ceramide synthesis. However, some recent research indicates that it is indeed implicated in several biological processes. They include activation of autophagy, cell cycle arrest and inhibition of ceramide induced channel formation in the mitochondria [4], thus mitigating the apoptotic effect of Cer [5].

3.1.4. Dihydroceramide Desaturase (DES1)

As previously seen in section 3.1.1., dihydroceramide desaturase (DES1) is the last enzyme in the *de novo* synthesis of Cer. It performs the insertion of a (*E*)-4 double bond into dhCer backbone to convert it to Cer. Therefore, DES1 regulates the dhCer/Cer ratio.

The exhibited biological functions of both Cer and dhCer may suggest DES1 as a therapeutic target to adjust metabolic processes and prevent cancer, viral infections, obesity and insulin resistance [3].

Hence, investigation of DES1 inhibitors might lead to therapeutic treatments for these illnesses. For instance, Holland et al. demonstrated how DES1 inhibition in muscle cells performed in mice enhanced insulin sensitivity [6]. Following this research path, some active site directed inhibitors of DES1 have been described, such as GT11 [7] and XM462 [8]. Besides, some drugs and natural products also present inhibition activity over DES1, such as Fenretinide (4-HPR), a derivate of retinoic acid which has being proved to have inhibition action over DES1 and to enhance insulin signalling [9]. Furthermore, investigations on these topics lead to the discovery of a Δ^6-unsaturated inhibitor. It was observed that introducing a *trans* double bond in the C6 position of a dhCer resulted in a potent DES1 inhibitor [3].

3.2. GARCINOIC ACID BIOLOGICAL ACTIVITY

Garcinoic acid (GA), also known as *trans*-13'-carboxy-δ-tocotrienol, is a natural product found in *Garcinia kola* seeds, an African type of nuts which have several therapeutic properties. This plant is commonly used to treat different inflammation and oxidation health issues.

Given GA structural similarly to retinoic acid, γ-tocopherol and γ-tocotrienol (Fig. 4), it is appropriate to consider that it may also share their biological activity. Evidence demonstrate that

this group of compounds present inhibition activity over DES1 [9], as it was mentioned before regarding Fenretinide, which consists of a carbamide derivative with 4-aminophenol of retinoic acid. Therefore, an analogue of this derivative with GA was tested *in vitro* and it resulted to be an even more potent DES1 inhibitor. The challenge to face now lies on the *in vivo* study. Thus, ongoing investigations are addressed to its administration in mice presenting high-fat diet-induced NAFLD.

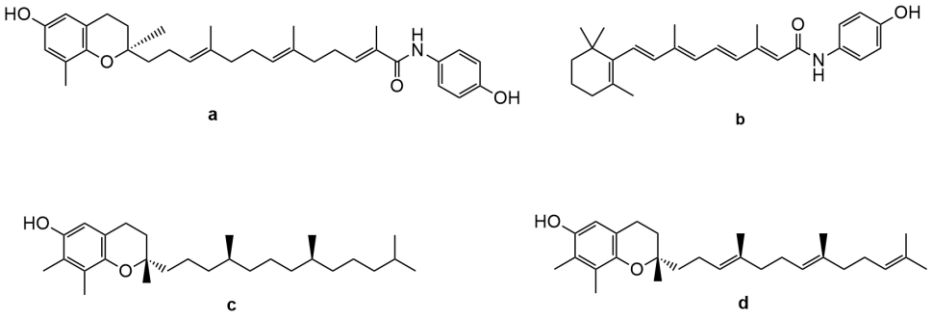

Figure 4.- *N*-(4-hydroxyphenyl)garcinamide (**a**), Fenretinide (**b**), γ-tocopherol (**c**) and γ-tocotrienol (**d**)

4. OBJECTIVES

It is clear that DES1, Cer and dhCer balance are therapeutic targets of great relevance in NAFLD and its progression to NASH, since accumulating evidence show their association with several pathologies related to this disease. Taking into consideration the previously discussed topics, further research in this field must be carried out in order to use these therapeutic tools.

Therefore, the objectives considered were the preparation of two compounds for the study of their inhibition activity on DES1. Concretely, the targets are a new class of inhibitors for hepatic cell cultures ((*E*)-Δ^6 ceramides) and the preparation at larger scale of a potential therapeutic drug (*N*-(4-hydroxyphenyl)garcinamide) to treat mice fed with a high-fat diet. The essential aims are:

1. Extraction of garcinoic acid from *Garcinia kola* seeds.
2. Preparation of 2 g of GA carbamide derivate, *N*-(4-hydroxyphenyl)garcinamide.
3. Implementation of a new pathway for the synthesis of a (*E*)-Δ^6 ceramide, *N*-((2*S*,3*R*,*E*)-1,3-dihydroxyoctadec-6-en-2-yl)pivaloylamide.

5. DERIVATIZATION OF GARCINOIC ACID

In order to achieve the preparation of the compound destinated to mice administration, it is essential to take into account that, although GA is a commercially available product, its price is not affordable (900€ per 20 mg). In this case, considering the yields of the coupling reaction with 4-aminophenol, at least 4 g of GA were needed. This fact makes its purchase unfeasible.

However, there is abundant literature for GA obtention and purification from natural sources (*Garcinia kola* seeds)[10]. Hence, GA was directly extracted from these seeds, The followed methodology consisted of several extractions with MeOH, its filtration and further purification using column chromatography.

5.1. *N*-(4-HYDROXYPHENYL)GARCINAMIDE SYNTHESIS

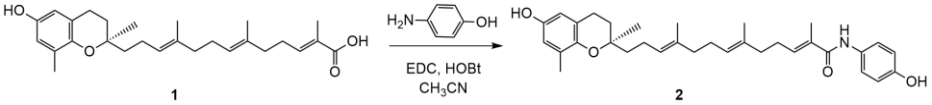

Figure 5.- Reaction of garcinoic acid into its *N*-aminophenol derivative

The preparation of this compound involves an acylation at the carboxy moiety of GA with 4-aminophenol. This was achieved by using an activating agent such as EDC, which forms a more electrophilic carbonyl group. Then, it can react with HOBt, a nucleophilic catalyst which avoids racemization. Thus, the attack of the 4-aminophenol is facilitated and the amide bond can be formed (Fig. 6). Since the presence of a small amount of base decreased the final yield, in this case no Et_3N was used as in other reaction done in our lab. While the reaction tends to last few hours in presence of base, the time needed in this case was at least two days.

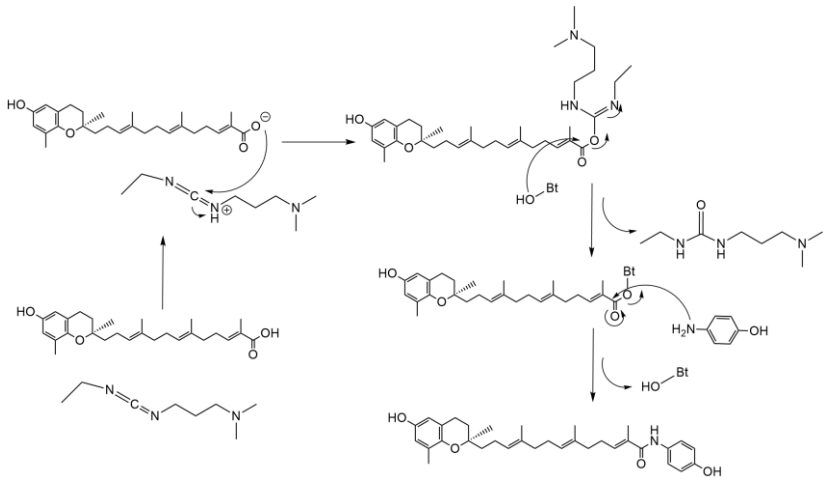

Figure 6.- Mechanism of garcinoic acid acylation

The attack of the alcohol from the 4-aminophenol could have also been possible, forming a carboester bond instead of the carbamide, since it is a nucleophilic agent. Despite this, it has been described how the use of EDC favours the N-acylation in front of the O-acylation [11]. Finally, the quantity obtained of both GA and its derivative was the desired one, 2 g each.

With the purpose of verifying that the obtained product was the carbamide, the different spectra were analysed. Firstly, as it can be observed in the ^{1}H-NMR spectrum (Fig 7), there are three singlets that integrate to one proton between 8 and 5 ppm. Therefore, there is the possibility for them to correspond to both alcohols protons and the amide proton that result when the *N*-acylation takes place. For this to be proved, one must examine the HSQC spectrum (Fig 8), since it describes the relation between the protons and their correspondent carbon. Hence, it can be noted that all the mentioned three protons do not have relation with any carbon signals and, consequently, they belong to the alcohols and amide.

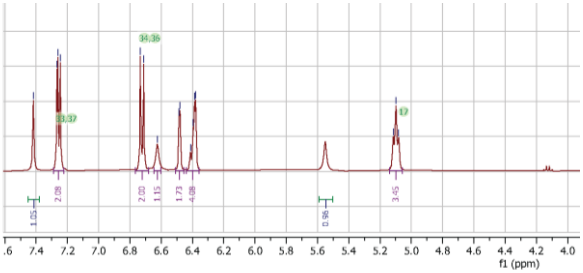

Figure 7.- ^{1}H-NMR spectrum of *N*-(4-Hydroxyphenyl)garcinamide

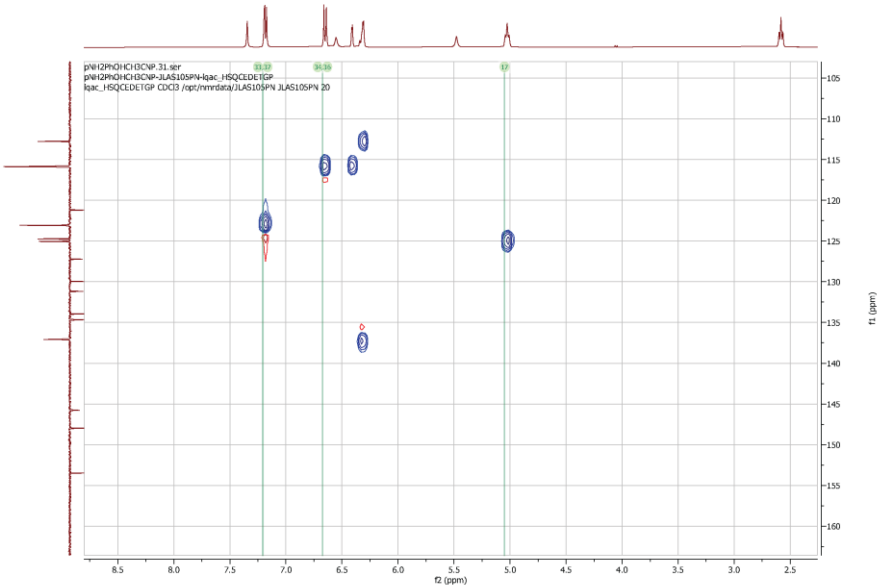

Figure 8.- HSQC spectrum of *N*-(4-Hydroxyphenyl)garcinamide

If the carboester had been formed, one of these three signals should have integrated to two, corresponding to the amine that would not have formed the amide bond.

Another alternative to ensure the carbamide formation is the protection of the alcohols groups as trimethylsilyl esters (TMS) [12].

6. (*E*)-Δ^6 CERAMIDES SYNTHESIS

A pathway for (*E*)-Δ^6 ceramides synthesis was already described by Pou et al. [3]. This synthetic route starts with Garner's aldehyde coupling with 3-butenylMgBr, followed by a sequence of reactions to finally afford two (*E*)-Δ^6 ceramides with different fatty acid substituents (Fig. 9).

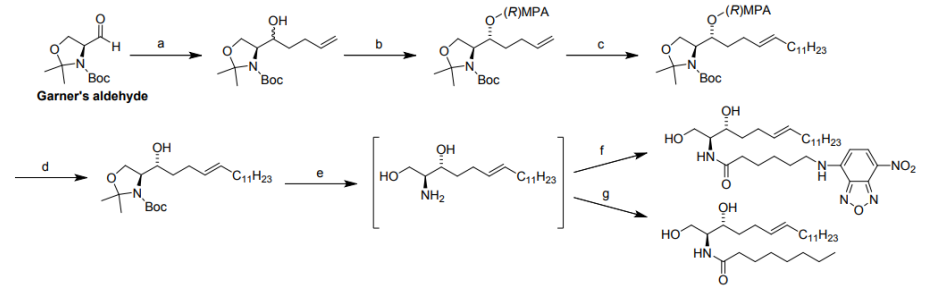

Figure 9.- Synthetic route for (*E*)-Δ^6 ceramides [3]. (a) 3-butenylMgBr, THF; (b) (R)-(-)-MPA, EDC, DMAP, CH_2Cl_2; (c) n-tridecene, Grubbs, 2nd generation, CH_2Cl_2; (d) K_2CO_3, MeOH; (e) AcCl, MeOH; (f) C6NBD acid, HOBt, EDC, CH_2Cl_2; (g) octanoic acid, HOBt, EDC, CH_2Cl_2

One of the downsides of this route is that in the first step, consisting of the coupling between the aldehyde and the 3-butenylMgBr into the alcohol formation, both enantiomers are obtained. This fact not only implies the loss of a considerable part of the product, but also the need of an additional step in order to separate both enantiomers, consisting in the derivatization with (*R*)-(-)-α-methoxy-α-phenylacetic acid.

Therefore, on view of these drawbacks, another equivalent route was proposed in which the starting material was the Weinreb amide of Garner's aldehyde (Fig 10). This alternative has the advantage that, during the coupling with the butenyl, a ketone instead of an enantiomer mixture is formed. Furthermore, the methodology to achieve the alcohol is through a diastereoselective reduction using $LiAlH(O^tBu)_3$.

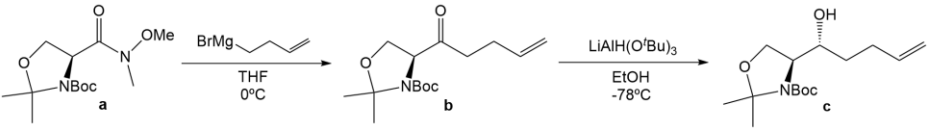

Figure 10.- Alternative synthesis

This pathway, however, presented a very low yield (6.6%) in the first reaction and the formation of an unknown by-product. Hence, another starting material (**3**) was used to carry out the final route.

The synthetic route followed to perform the (*E*)-Δ^6 ceramide (**8**) preparation is detailed (Fig. 11). It consists in a linear route which implies two critical stereochemical points; the creation of a new chiral centre (ketone reduction) and the cross-metathesis reaction.

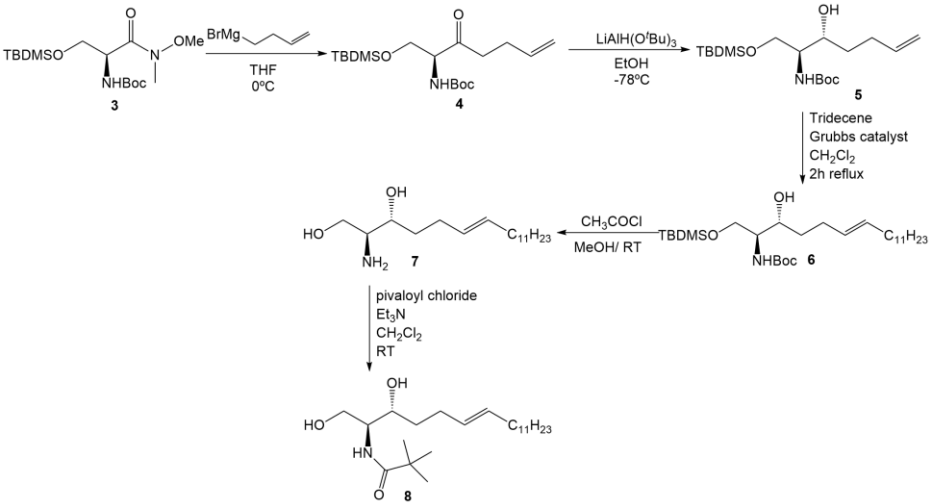

Figure 11.- Synthetic route for *N*-((2*S*,3*R*,*E*)-1,3-dihydroxyoctadec-6-en-2-yl)pivaloylamide preparation

6.1. KETONE FORMATION: GRIGNARD REACTION

It is known that Weinreb amides are one of the most relevant amides derivatives. This is due to their capability of forming five-membered chelates, which stabilizes the intermediate, so that the ketone cannot undergo a second addition, and can successfully form high-functionalized ketones and aldehydes through nucleophilic addition of organomagnesium reagents [13][14]. The formation of the ketone is not completed until the quenching process, in which mild aqueous acid conditions are needed to prevent the deprotection of any of both protective groups. The detailed mechanism is depicted (Fig. 12).

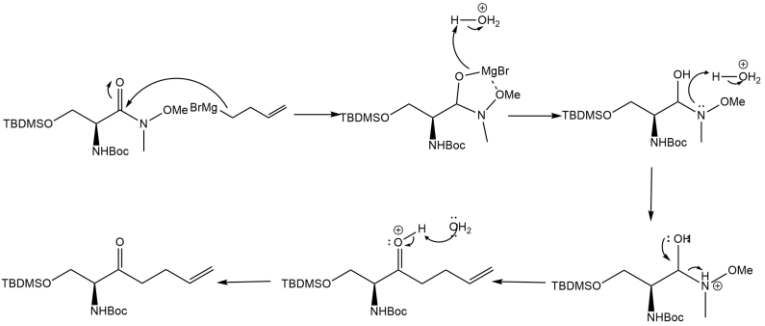

Figure 12.- Mechanism of ketone **4** formation

6.2. DIASTEREOSELECTIVE KETONE REDUCTION

Reduction of ketones and aldehydes is a commonly used strategy to synthesize alcohols. The accepted method to perform this transformation is the use of active hydride reagents. The universal one is lithium hydride ($LiAlH_4$), capable of reducing from ketones to nitriles. However, its incapability to tolerate other groups and its high reactivity requires the employment of milder and more selective reagents, such as $LiAlH(O^tBu)_3$ to increase selectivity. This hydride is able to reduce ketones and aldehydes, transferring just one proton to the carbonyl, the other one required must come from the solvent, in this case ethanol (Fig. 13).

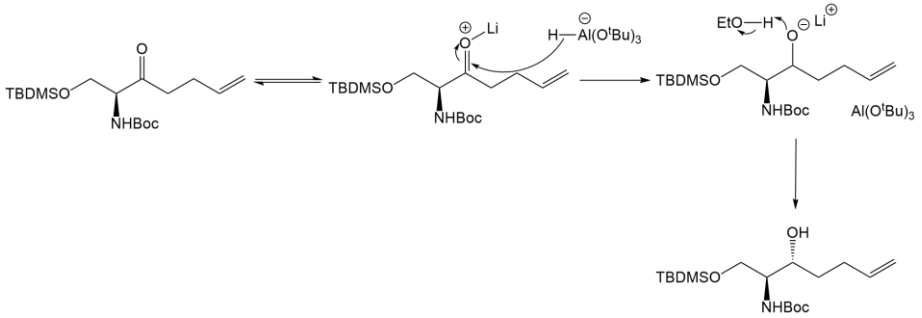

Figure 13.- Diastereoselective reduction mechanism

This reaction follows the chelation Cram model (Fig. 14) were the hydride, by way of the Bürgi-Dunitz trajectory, attacks the more sterically favoured face of the compound and, consequently, forms the *anti* isomer, which is the desired product. Otherwise, if the reaction followed the Felkin-Anh model, the obtained product would have been the *syn* isomer.

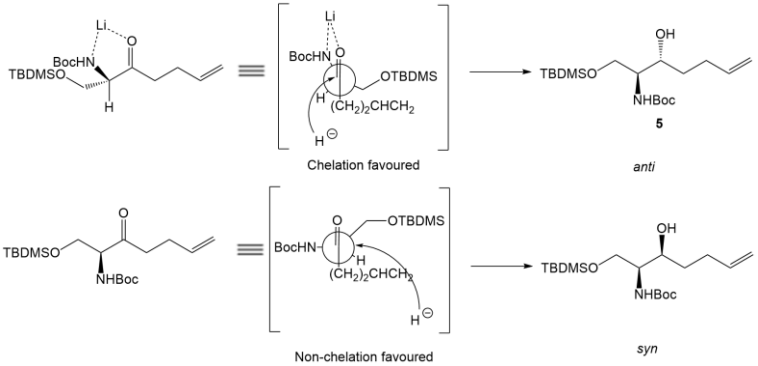

Figure 14.- Chelation Cram and Felkin-Anh models

This strategy is the properly to adopt in this particular case since a more reactive hydride as $LiAlH_4$ would have reduced the ester in the Boc protective group. Therefore, following the described method it is possible to simply react with the ketone to form the desired alcohol.

Considering that a new chiral centre is being formed during this reaction, it is essential to determine the absolute configuration of the product. This can be accomplished by the derivatization of the alcohol into two different esters (diastereomers) using both enantiomers of methoxyphenylacetic acid (MPA). Each derivative presents their own distinctive NMR spectra. Through its examination it is possible to deduce the configuration by the differences between their chemical shifts and its comparison with an empirical model [15]. In this model it is described that the phenyl ring can provoke a distinction in the chemical shifts depending on which configuration does MPA has (*R* or *S*). Hence, in (*R*)-MPA ester, substituent L_1 (Fig. 15) is shielded (lower chemical shifts) while L_2 remains unaltered, whereas in the (*S*)-MPA ester the L_2 group is the shielded one. Therefore, alcohols showing $\Delta\delta^{RS} L_1 < 0$ and $\Delta\delta^{RS} L_2 > 0$, will present *R* configuration if the substituent placed in L_1 is the second group, following the Cahn-Ingold-Prelog rules.

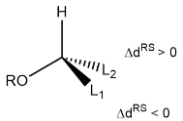

Figure 15.- Model for configurational correlation of MPA esters[15]

Results in Table 1, processing them with the explained model, determine the configuration of the alcohol to be *R*.

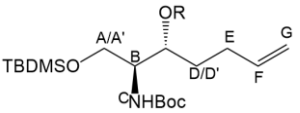

	δH_A	$\delta H_{A'}$	δH_B	δH_C	δH_D	$\delta H_{D'}$	δH_E	δH_F	δH_G
R = (*R*)-MPA	3.30	3.04	3.66	4.46	2.04	2.04	1.67	5.75	4.93
R = (*S*)-MPA	3.57	3.57	3.86	4.80	1.63	1.63	1.56	5.53	4.86
$\Delta\delta^{RS}$	-0.27	-0.53	-0.20	-0.34	0.41	0.41	0.11	0.22	0.07

(a) Chemical shifts (δ) are reported in ppm relative to the solvent signal

Table 1.- Absolute configuration determination of alcohol **5**

6.3. OLEFINATION: CROSS-METATHESIS REACTION

Cross-metathesis is a catalytic (1-5 mol%), reversible and with high levels of regio, chemo and stereoselectivity process and it represents a resourceful tool for C-C bond formation. Its reversible character usually implies an *E* olefin formation. The mechanism of this reaction is depicted in Fig. 16 and it starts with a [2+2] cycloaddition reaction between the catalyst (metal carbene, **III**) and one of the olefins to form a metallacyclobutane (**IV**). This latest one experiences a rearrangement to achieve a new metal carbene (**I**), which reacts with the other olefin to, similarly, yield the desired product [16].

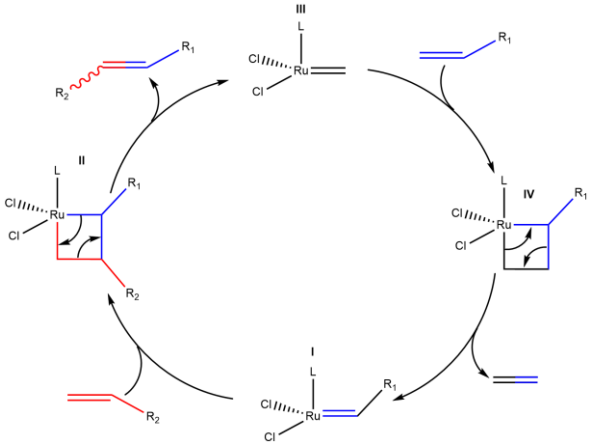

Figure 16.- Cross-metathesis mechanism

This mechanism implies not only the formation of the desired product, but also the obtainment of several by-products due to the catalyst action. These includes all the possibilities of the homocoupling olefins and its *Z* isomers. Analysing the NMR spectra, it was not possible to discern whether the obtained isomer corresponded to the *E* or *Z* isomer; due to the overlapping of the signals from the double bond hydrogens, the determination of the coupling constants was not attainable. However, during column chromatography it was assumed that the major product was the *E* stereoisomer since it is the more thermodynamically stable one [17].

6.4. *N*-Boc and TBDMS deprotection

In order to perform the removal of the Boc and TBDMS protective groups, there are different alternatives, such as trifluoroacetic acid, metal catalysis, deprotection with HCl in organic solvents [18] or with acetyl chloride in MeOH [19], which is the chosen one. This strategy generates HCl through an acyl nucleophilic substitution (Fig. 17).

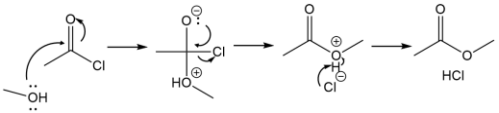

Figure 17.- *In situ* generation of HCl

The production of HCl *in situ* allows the removal of both TBDMS and Boc groups with the formation of isobutylene and carbon dioxide, detailed in Fig. 18.

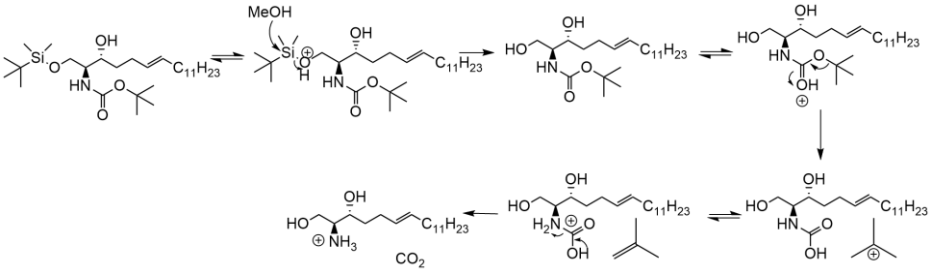

Figure 18.- TBDMS and Boc deprotection mechanism

It is important to perform a basic treatment after the reaction has been completed in order to release the protonated amine.

Regarding the deprotection of the TBS ethers there also exist a variety of strategies. These go from employing chloro compounds like cerium chloride, TMSCl in H_2O or LiCl in DMF; to the use of I_2, Oxone in methanol and DDQ [20]. The problem is that the use of some of these methods implies harsh conditions, incompatibility with other protective groups (thio group at the anomeric position), overoxidation, etc [20]. Therefore, a milder method such as acetyl chloride in methanol is preferable.

6.5. SPHINGOSINE ACYLATION

The final step of the synthesis requires the acylation of the amine from the sphingosine. In view of that the reagent for this reaction was pivaloyl chloride, there was no necessity of activating agents due to its high reactivity. Consequently, the reaction was carried out merely in presence of triethylamine (Et_3N). The mechanism is detailed in Fig. 19. The final product **8** was obtained in a quantity of 20 mg. It was characterized through ^{1}H-NMR and its exact mass determined by FIA-HRMS.

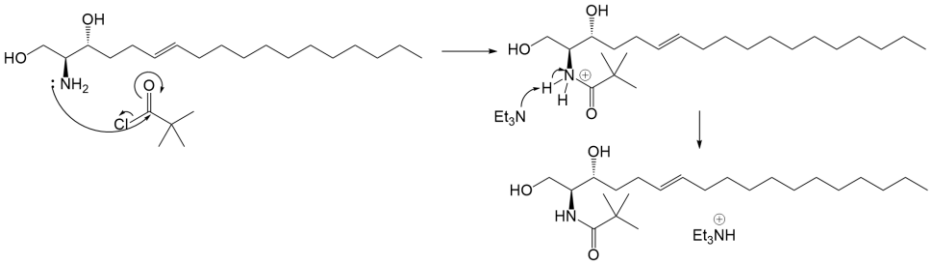

Figure 19.- Mechanism of sphingosine acylation

7. EXPERIMENTAL SECTION

7.1. MATERIALS AND METHODS

Most of the reagents were acquired from Sigma-Aldrich and Acros and employed without further purification. All reactions were followed by TLC analysis using MERCK® TLC Silicagel 60G F254. UV light (265 nm) was used as visualizing agent and a 5% (w/v) solution of phosphomolybdic acid in ethanol was used as staining agent. Products were purified by flash column chromatography with Sigma-Aldrich silica gel (pore size 60 Å, particle size 40-60μm) as stationary phase. Gradients of the mobile phase are specified for each compound.

NMR spectra were registered at room temperature (RT) with a 400 MHz Bruker NMR spectrometer. Chemical shifts (δ) are described in ppm relative to the solvent signal in ^{1}H-NMR and coupling constants (J) in Hz. The following abbreviations are used to define the multiplicity in ^{1}H-NMR spectra: s = singlet, brs = broad singlet, d = doublet, dd = doublet of doublets, t = triplet, dt = doublet of triplets, ddt = doublet of doublet of triplets, dq = doublet of quadruplets, m = multiplet, dm = double of multiplets. FIA-HRMS analysis was carried out with Waters Bioaccord LC-MS system.

7.2. PREPARATION OF N-(4-HYDROXYPHENYL)GARCINAMIDE

7.2.1. Extraction of Garcinoic acid (1) from *Garcinia kola* seeds

Seeds of Garcinia kola (989 g) were grounded and extracted with MeOH (2 L x 5) at RT. The obtained extract was then washed with acidified water and evaporated under reduced pressure to achieve a brownish oil, which was purified by flash column chromatography using hexane/ EtOAc and eluting with a 1% gradient increase of EtOAc up to 45%. A dark brown oil was recovered (**1**, 10.81 g, 1.09% yield).

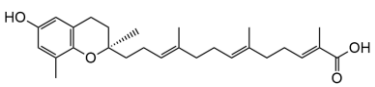

1

Compound **1:** Brown oil. ^{1}H NMR ($CDCl_3$, 400 MHz): δ 6.93-6.83 (m,1H), 6.48 (d, J = 3.0 Hz, 2H), 6.38 (d, J = 3.0 Hz, 2H), 5.12 (t, J = 7.0 Hz, 4H), 2.69 (t, J = 7.0 Hz, 3H), 2.28 (q, J = 7.0 Hz, 3H), 2.16-2.03 (m, 16H), 2.01-1.95 (m, 4H), 1.83 (s, 4H), 1.75 (ddd, J = 20.0, 14.0, 6.5 Hz, 4H), 1.59 (d, J = 3.0 Hz, 13H), 1.26 (s, 4H).

7.2.2 Synthesis of *N*-(4-hydroxyphenyl)garcinamide (2)

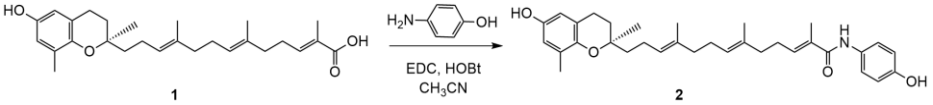

Figure 20.- GA acylation reaction

In a 250 mL round-bottom flask, 1 g (2.34 mmol) of garcinoic acid, 0.307 g (2.81mmol) of 4-aminophenol and 0.431 g (2.8 mmol) of HOBt were dissolved in 48 mL of anhydrous CH_3CN. The solution was brought under Ar atmosphere and 0.719 g (3.75 mmol) of EDC were added while stirring. The mixture was maintained under constant stirring for 2 days at RT.

Then, the reaction crude was extracted with CH_2Cl_2 (15 mL x 3) and washed with water. The collected organic phases were evaporated under reduced pressure in order to remove the solvent and the residue was purified by flash column chromatography. The eluents used were hexane/EtOAc with a 2% gradient of EtOAc up to 75%.

The product showed little impurities when eluted in TLC using CH_2Cl_2/ MeOH 95:5. Therefore, a repurification was carried out by column chromatography eluting with CH_2Cl_2/MeOH using a 0.1% gradient of MeOH up to 3.6%. A brown oil was obtained (**2**, 1.992 g, 54.71% yield).

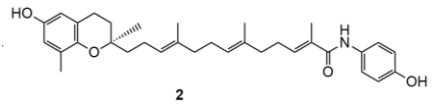

Compound **2**: Brown oil. ^{1}H NMR ($CDCl_3$, 400 MHz): δ 7.26 (d, *J* = 9.0 Hz, 2H), 6.72 (d, *J* = 9.0 Hz, 2H), 6.62 (s, 1H), 6.48 (d, *J* = 3.0 Hz, 2H), 6.39 (dd, J =8.0, 5.0 Hz, 4H), 5.10 (t, *J* = 7.0 Hz, 3H), 2.66 (t, *J* = 7.0 Hz, 3H), 2.22 (p, *J* = 9.0, 8.0 Hz, 3H), 2.13-2.00 (m, 16H), 1.97 (t, *J* = 7.0 Hz, 4H), 1.91 (s, 4H), 1.84-1.67 (m, 5H), 1.58 (d, *J* = 5.0 Hz, 10H), 1.26 (s, 4H).

7.3. (*E*)-Δ^6 CERAMIDES SYNTHESIS

7.3.1. Preparation of 3-butenylmagnesium bromide

1.44 g (60 mmol) of magnesium, previously washed with acid, were weighted and dried in a 250 mL round bottom flask. 100 mL of anhydride ether were introduced and 0.5 mL of a 1M DIBALH solution were added under Ar atmosphere and constant stirring, whose function is to

remove moisture, alcohols and peroxides formed by oxygen. Then, 3 mL (30 mmol) of 4-bromo-1-butene were added dropwise to the mixture. A grey solution was obtained.

7.3.2. Synthesis of *tert*-butyl (*S*)-2,2-dimethyl-4-(pent-4-enoyl)oxazolidine-3-carboxylate

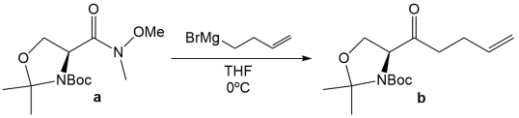

Figure 21.- Grignard reaction

To an ice-cold solution of 0.6 g (2 mmol) of the Wenreib amide in 5 mL of THF was added dropwise 10 mL (5 mmol) of the previously prepared 3-butenylmagnesium bromide. The mixture was stirred at the same temperature for 3 hours. Afterwards, the reaction was quenched with 10 mL of a solution of citric acid-HCl 6:4 and extracted with EtOAc (3x15 mL). The organic phases were combined and evaporated under reduced pressure to obtain a yellowish oil, which was purified with column chromatography using hexane/ EtOAc as eluents and a gradient of 0.5% of EtOAc up to 10.5-14%. A colourless oil was recovered (**b**, 40 mg, 6.6% yield).

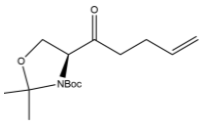

Compound **b**: Yellowish oil. ^{1}H NMR ($CDCl_3$, 400 MHz): δ 5.95–5.69 (m, 1H), 5.11–4.90 (m, 2H), 4.51–4.26 (m, 1H), 4.20–4.06 (m, 1H), 3.97–3.85 (m, 1H), 2.71–2.49 (m, 2H), 2.34 (m, 2H), 1.68 (d, J = 24.0 Hz, 2H), 1.50 and 1.41 (2s, 12H).

7.3.3. *Tert*-butyl (*S*)-(1-((*tert*-butyldimethylsilyl)oxy)-3-oxohept-6-en-2-yl)carbamate synthesis (4)

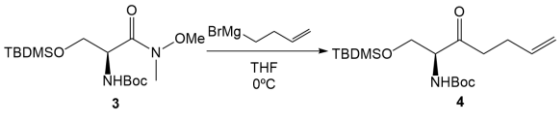

Figure 22.- Grignard reaction with **3** as starting material

In a 250 mL round-bottom flask, 2.7 g (7.5 mmol) of the Wenreib amide **3** were introduced and dissolved in 50 mL of THF. The solution was cooled down to -30ºC and 100 mL (50 mmol) of a freshly prepared solution of butenylmagnesium bromide were added dropwise with constant

stirring. The reaction was then left to warm up to RT and quenched with a citric acid-HCl 6:4 solution before performing an extraction with EtOAc (3x50 mL). The organic fractions were put together and the solvents were evaporated under reduced pressure. The residue obtained was finally purified with column chromatography, hexane/ EtOAc were the solvents used to elute the product using a 1% gradient up to 16-20% of EtOAc. It was obtained a yellowish oil (**4**, 240 mg, 9% yield).

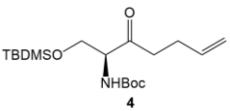

4

Compound **4**: Yellowish oil. ^{1}H NMR ($CDCl_3$, 400 MHz) δ 5.80 (ddt, J = 17.0, 10.0, 6.5 Hz, 1H), 5.47 (d, J = 7.0 Hz, 1H), 5.00 (dq, J = 17.0, 1.5 Hz, 1H), 4.94 (dm, 1H), 4.26 (m, 1H), 4.06 (dd, J = 10.0, 3.0 Hz, 1H), 3.81 (dd, J = 10.0, 3.0 Hz, 1H), 2.71 (dt, J = 17.5, 7.5 Hz, 1H), 2.57 (dt, J = 17.5, 7.5 Hz, 1H), 2.34 (m, 2H), 1.45 (s, 9H), 0.85 (s, 9H), 0.03 (s, 6H). FIA-HRMS (ESI): m/z calc. for $C_{13}H_{27}NO_2Si^+$ $[M+H]^+$ 258.1811; found 258.1807.

7.3.4. Synthesis *tert*-butyl ((2*S*,3*R*)-1-((*tert*-butyldimethylsilyl)oxy)-3-hydroxyhept-6-en-2-yl)carbamate (5)

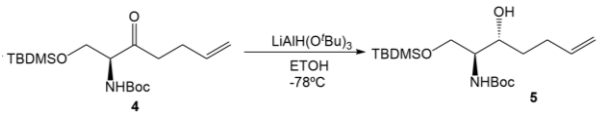

4 **5**

Figure 23.- Diastereoselective reduction

In a 250 mL round-bottom flask, 1.6 g (6.25 mmol) of $LiAlH(O^tBu)_3$ and 30 mL of absolute ethanol were introduced and cooled down to -78 ºC. To this stirring mixture, 880 mg (2.5 mmol) of **4** were added dropwise under Ar atmosphere.

The day after, the resulting solution was quenched with 8 mL of a 10% citric acid solution and extracted with EtOAc. Then, it was evaporated under reduced pressure and finally purified by using column chromatography. The eluents used were hexane/ EtOAc with a 0.5% of EtOAc gradient up to 11-13%. A colourless oil was recovered (**5**, 564 mg, 64% yield).

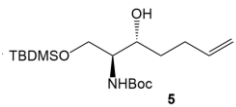

5

Compound **5:** Colourless oil. ^{1}H NMR ($CDCl_3$, 400 MHz) δ 5.84 (ddt, J = 17.0, 10.0, 6.5 Hz, 1H), 5.29 (d, J = 7.2, 1H), 5.00 (dq, J = 17.0, 1.5 Hz, 1H), 4.94 (dm, 1H), 3.96 (dd, J = 10.5, 3.0 Hz, 1H), 3.82 (dd, J = 10.0, 3.0 Hz, 1H), 3.72–3.62 (m, 1H), 3.52 (s, 1H), 2.39–2.25 (m, 1H), 2.21–2.08 (m, 1H), 1.69–1.57 (m, 2H), 1.45 (s, 9H), 0.90 (s, 9H), 0.08 (s, 6H).

7.3.5. *Tert*-butyl ((2*S*,3*R*,*E*)-1-((*tert*-butyldimethylsilyl)oxy)-3-hydroxyoctadec-6-en-2-yl)carbamate (6) preparation

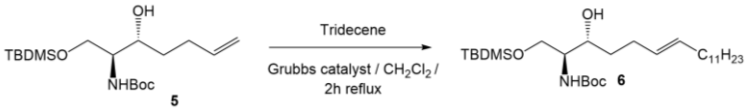

Figure 24.- Cross-metathesis reaction

560 mg (1.6 mmol) of **5** were introduced along with 1 mL (4.5 mmol) of tridecene in a 100 mL round-bottom flask and dissolved in 20 mL of degasified CH_2Cl_2. 70 mg of the second generation Grubbs catalyst were added and the mixture was refluxed for 5 hours. Afterwards, the organic solvents were evaporated under reduced pressure and the dark red residue obtained was purified with column chromatography using hexane/ EtOAc as eluents and a 0.4% gradient of EtOAc up to 6-8%. A colourless oil was achieved (**6**, 144 mg, 20% yield).

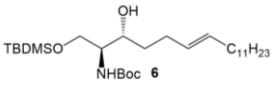

Compound **6**: Colourless oil. ^{1}H NMR ($CDCl_3$, 400 MHz) δ 5.43 (m, 2H), 5.29 (d, J = 5.5 Hz, 1H), 3.95 (dd, J = 10.5, 3.0 Hz, 1H), 3.81 (d, J = 10.5 Hz, 1H), 3.68–3.60 (m, 1H), 3.50 (s, 1H), 2.29–2.16 (m, 1H), 2.13–2.01 (m, 1H), 1.97 (q, J = 6.5 Hz, 2H), 1.63–1.54 (m, 2H), 1.45 (s, 9H), 1.26 (s, 18H), 0.90 (s, 9H), 0.87 (t, J = 7.0 Hz, 3H), 0.08 (s, 6H).

7.3.6. Synthesis of (2*S*,3*R*,*E*)-2-aminooctadec-6-ene-1,3-diol (7)

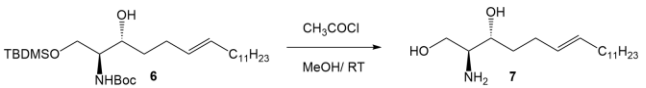

Figure 25.- Deprotection reaction

In a 100 mL round-bottom flask, 144 mg (0.3 mmol) of **6** and 0.1 mL (1.5 mmol) of CH_3COCl were dissolved in 15 mL of MeOH. The mixture was stirred at RT overnight. The day after, the reaction crude was evaporated under reduced pressure and washed with MeOH and a 30% NH_3 solution. The residue obtained was purified with column chromatography using CH_2Cl_2 and MeOH with a gradient up to 13-17% of MeOH. A colourless solid was afforded (**7**, 83 mg, 98% yield)

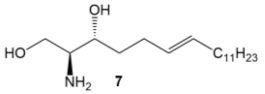

Compound **7**: Colourless solid. ^{1}H NMR (400 MHz, Methanol-d_4) δ 5.60–5.36 (m, 2H), 3.90–3.78 (m, 2H), 3.76–3.67 (m, 1H), 3.27–3.18 (m, 1H), 2.31–2.18 (m, 1H), 2.15–2.06 (m, 1H), 1.99 (q, J = 6.5 Hz, 2H), 1.55 (q, J = 7.5 Hz, 2H), 1.31 (s, 18H), 0.90 (t, J = 7.0 Hz, 3H). FIA-HRMS (ESI): m/z calc. for $C_{18}H_{37}NO_2^+$ [M+H]$^+$ 300.2824; found 300.2819.

7.3.7. Synthesis of *N*-((2*S*,3*R*,*E*)-1,3-dihydroxyoctadec-6-en-2-yl)pivaloylamide (8)

Figure 26.- Sphingosine acylation

In a 50 mL round-bottom flask, 40 mg (0.13 mmol) of dried **9** were introduced and dissolved in anhydrous CH_2Cl_2. To this stirring solution, 56 µL (0.4 mmol) of Et_3N were inserted previously the dropwise addition of 15.6 µL (0.13 mmol) of pivaloyl chloride. The mixture was stirred at RT for 1 hour and, after its finalization, it was dissolved in 10 mL of CH_2Cl_2 and 2 mL of water was added. Then, the crude was extracted with EtOAc. Combined organic layers were evaporated under reduced pressure to finally purified by means of column chromatography. The eluents used were CH_2Cl_2/ MeOH with a 0.5 % gradient of MeOH up to 5%. It resulted in a white solid obtention (**8**, 23 mg, 46% yield).

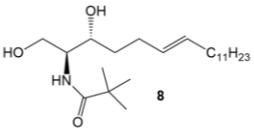

Compound **8**: White solid. ^{1}H NMR ($CDCl_3$, 400 MHz) δ 6.55 (d, J = 7.5 Hz, 1H), 5.54–5.33 (m, 2H), 3.97 (dd, J = 11.5, 3.0 Hz, 1H), 3.82–3.74 (m, 1H), 3.71 (dd, J = 11.5, 3.0 Hz, 1H), 2.26–2.13 (m, 1H), 2.13–2.05 (m, 1H), 1.96 (q, J = 6.5 Hz, 2H), 1.68–1.51 (m, 2H), 1.25 (s, 18H), 1.21 (s, 9H), 0.87 (t, J = 7.0 Hz, 3H). FIA-HRMS (ESI): m/z calc. for $C_{23}H_{45}NO_3^+$ [M+H]$^+$ 384.3399; found 384.3401.

7.3.8. Derivatization of *tert*-butyl ((2*S*,3*R*)-1-((*tert*-butyldimethylsilyl)oxy)-3-hydroxyhept-6-en-2-yl)carbamate

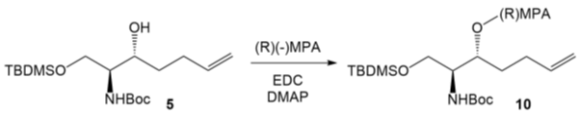

Figure 27.- Derivatization reaction

A solution of (*R*)-(-)-α-methoxy-α-phenylacetic acid, EDC and DMAP in anhydrous CH_2Cl_2 was added dropwise to a solution of 5 under argon atmosphere. The mixture was stirred at RT for 7 hours and washed with HCl, saturated $NaHCO_3$ and water. At that point it was dried over $MgSO_4$ and the solvent was evaporated under reduced pressure to be finally purified with column chromatography using hexane/EtOAc 90:10.

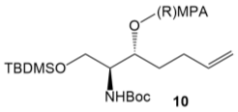

10

Compound **10**: ^{1}H NMR ($CDCl_3$, 400 MHz) *δ* 5.75 (ddt, *J* = 17.0, 10.0, 6.5 Hz, 1H), 5.07–5.00 (m, 1H), 4.95 (d, *J* = 1.5 Hz, 1H), 4.74 (s, 1H), 4.46 (d, *J* = 9.5 Hz, 1H), 3.68 (br s, 1H), 3.41 (s, 3H), 3.31 (dd, *J* = 10.0, 4.0 Hz, 1H), 3.04 (dd, *J* = 10.0, 4.0 Hz, 1H), 2.16–1.94 (m, 2H), 1.41 (s, 9H), 0.82 (s, 9H), -0.11 (s, 6H).

8. CONCLUSIONS

Within this work it has been achievable to:

1. Extract GA from *Garcinia kola* seeds.
2. Escalate the preparation of GA derivate, *N*-(4-hydroxyphenyl)garcinamide, up to 2 g for its administration in mice fed with high-fat diet.
3. Develop and implement a new synthetic route for (*E*)-Δ^6 ceramides preparation.
4. Imply and ensure a stereochemical control in the reduction stage of this new methodology.
5. Prove the stereochemical control through the determination of the absolute configuration.
6. By means of this alternative route, synthesize a new inhibitor of (*E*)-Δ^6 ceramides class, *N*-((2*S*,3*R*,*E*)-1,3-dihydroxyoctadec-6-en-2-yl)pivaloylamide, whose inhibition activity on DES1 will be tested over hepatic cell cultures.

9. REFERENCES AND NOTES

1. Régnier, M.; Polizzi, A.; Guillou, H.; Loiseau, N. Sphingolipid Metabolism in Non-Alcoholic Fatty Liver Diseases. *Biochimie* **2019**, *159*, 9–22, doi:10.1016/j.biochi.2018.07.021.
2. Pagadala, M.; Kasumov, T.; McCullough, A.J.; Zein, N.N.; Kirwan, J.P. Role of Ceramides in Nonalcoholic Fatty Liver Disease. *Trends Endocrinol. Metab.* **2012**, *23*, 365–371, doi:10.1016/j.tem.2012.04.005.
3. Pou, A.; Abad, J.L.; Ordóñez, Y.F.; Garrido, M.; Casas, J.; Fabriàs, G.; Delgado, A. From the Configurational Preference of Dihydroceramide Desaturase-1 towards Δ6-Unsaturated Substrates to the Discovery of a New Inhibitor. *Chem. Commun.* **2017**, *53*, 4394–4397, doi:10.1039/c6cc08268h.
4. Rodriguez-Cuenca, S.; Barbarroja, N.; Vidal-Puig, A. Dihydroceramide Desaturase 1, the Gatekeeper of Ceramide Induced Lipotoxicity. *Biochim. Biophys. Acta - Mol. Cell Biol. Lipids* **2015**, *1851*, 40–50, doi:10.1016/j.bbalip.2014.09.021.
5. Fabrias, G.; Muñoz-Olaya, J.; Cingolani, F.; Signorelli, P.; Casas, J.; Gagliostro, V.; Ghidoni, R. Dihydroceramide Desaturase and Dihydrosphingolipids: Debutant Players in the Sphingolipid Arena. *Prog. Lipid Res.* **2012**, *51*, 82–94, doi:10.1016/j.plipres.2011.12.002.
6. Holland, W.L.; Brozinick, J.T.; Wang, L.P.; Hawkins, E.D.; Sargent, K.M.; Liu, Y.; Narra, K.; Hoehn, K.L.; Knotts, T.A.; Siesky, A.; et al. Inhibition of Ceramide Synthesis Ameliorates Glucocorticoid-, Saturated-Fat-, and Obesity-Induced Insulin Resistance. *Cell Metab.* **2007**, *5*, 167–179, doi:10.1016/j.cmet.2007.01.002.
7. Triola, G.; Fabrias, G.; Dragusin, M.; Niederhausen, L.; Broere, R.; Llebaria, A.; Echten-deckert, G. Van Specificity of the Dihydroceramide Desaturase Inhibitor N- Cyclopropenyl) Ethyl] Octanamide (GT11) in Primary Cultured Cerebellar Neurons. *Lipids* **2004**, *66*, 1671–1678, doi:10.1124/mol.104.003681.amide.
8. Munoz-Olaya, J.M.; Matabosch, X.; Bedia, C.; Egido-Gabás, M.; Casas, J.; Llebaria, A.; Delgado, A.; Fabriàs, G. Synthesis and Biological Activity of a Novel Inhibitor of Dihydroceramide Desaturase. *ChemMedChem* **2008**, *3*, 946–953, doi:10.1002/cmdc.200700325.
9. Casasampere, M.; Ordoñez, Y.F.; Pou, A.; Casas, J. Inhibitors of Dihydroceramide Desaturase 1: Therapeutic Agents and Pharmacological Tools to Decipher the Role of Dihydroceramides in Cell Biology. *Chem. Phys. Lipids* **2016**, *197*, 33–44, doi:10.1016/j.chemphyslip.2015.07.025.
10. Wallert, M.; Bauer, J.; Kluge, S.; Schmölz, L.; Chen, Y.C.; Ziegler, M.; Searle, A.K.; Maxones, A.; Schubert, M.; Thürmer, M.; et al. The Vitamin E Derivative Garcinoic Acid from Garcinia Kola Nut Seeds Attenuates the Inflammatory Response. *Redox Biol.* **2019**, *24*, 101166, doi:10.1016/j.redox.2019.101166.
11. Um, S.J.; Kwon, Y.J.; Han, H.S.; Park, S.H.; Park, M.S.; Rho, Y.S.; Sin, H.S. Synthesis and Biological Activity of Novel Retinamide and Retinoate Derivatives. *Chem. Pharm. Bull.* **2004**, *52*, 501–506, doi:10.1248/cpb.52.501.

12. Bruice, P.Y. *Organic Chemistry*; Pearson Education, 2016; ISBN 9780134042282.

13. Li, G.; Szostak, M. Synthesis of Biaryl Ketones by Arylation of Weinreb Amides with Functionalized Grignard Reagents under Thermodynamic Controlvs.Kinetic Control OfN,N-Boc2-Amides. *Org. Biomol. Chem.* **2020**, *18*, 3827–3831, doi:10.1039/d0ob00813c.

14. Murphy, J.A.; Commeureuc, A.G.J.; Snaddon, T.N.; McGuire, T.M.; Khan, T.A.; Hisler, K.; Dewis, M.L.; Carling, R. Direct Conversion of N-Methoxy-N-Methylamides (Weinreb Amides) to Ketones via a Nonclassical Wittig Reaction. *Org. Lett.* **2005**, 7, 1427–1429, doi:10.1021/ol050337b.

15. Louzao, I.; Seco, J.M.; Quiñoá, E.; Riguera, R. The Assignment of Absolute Configuration of Cyanohydrins by NMR. *Chem. Commun.* **2006**, 1422–1424, doi:10.1039/b517917c.

16. Connon, S.J.; Blechert, S. Recent Developments in Olefin Cross-Metathesis. *Angew. Chemie - Int. Ed.* **2003**, *42*, 1900–1923, doi:10.1002/anie.200200556.

17. Luján, C.; Nolan, S.P. E/Z Selectivity in Ruthenium-Mediated Cross Metathesis. *Catal. Sci. Technol.* **2012**, *2*, 1027–1032, doi:10.1039/c2cy00457g.

18. George, N.; Ofori, S.; Parkin, S.; Awuah, S.G. Mild Deprotection of the: N-Tert -Butyloxycarbonyl (N -Boc) Group Using Oxalyl Chloride. *RSC Adv.* **2020**, *10*, 24017–24026, doi:10.1039/d0ra04110f.

19. Nudelman, A.; Bechor, Y.; Falb, E.; Fischer, B.; Wexler, B.A.; Nudelman, A. Acetyl Chloride-Methanol as a Convenient Reagent for: A) Quantitative Formation of Amine Hydrochlorides; B) Carboxylate Ester Formation; C) Mild Removal of N-t-Boc-Protective Group. *Synth. Commun.* **1998**, *28*, 471–474, doi:10.1080/00397919808005101.

20. Khan, A.T.; Mondal, E. A Highly Efficient and Useful Synthetic Protocol for the Cleavage of Tert-Butyldimethylsilyl (TBS) Ethers Using a Catalytic Amount of Acetyl Chloride in Dry Methanol. *Synlett* **2003**, 694–698, doi:10.1055/s-2003-38360.

10. ACRONYMS

Ar: argon

Boc: *tert*-butoxycarbonyl

Cer: ceramide

DhCer: dihydroceramide

DES1: Δ-4-dihydroceramide desaturase 1

EDC: *N*-(3-dimethylaminopropyl)-N'-ethylcarbodiimide

ER: endoplasmatic reticulum

Et_3N: triethylamine

EtOAc: ethyl acetate

FFA: free fatty acids

GA: garcinoic acid

HCl: clorhidric acid

HOBt: hidroxybenzotriazole

MeOH. Methanol

MPA: methoxyphenylacetic acid

NAFLD: non-alcoholic fatty liver disease

PP2A: phosphatase 2A

TAGs: triacylglycerols

TNF-α: tumor necrosis factor α

SL: Sphingolipid

SMase: sphingomyelinase

S1P: sphingosine-1-phosphate

SPT: palmitoyltransferase

APPENDICES

APPENDIX 1: NMR SPECTRA

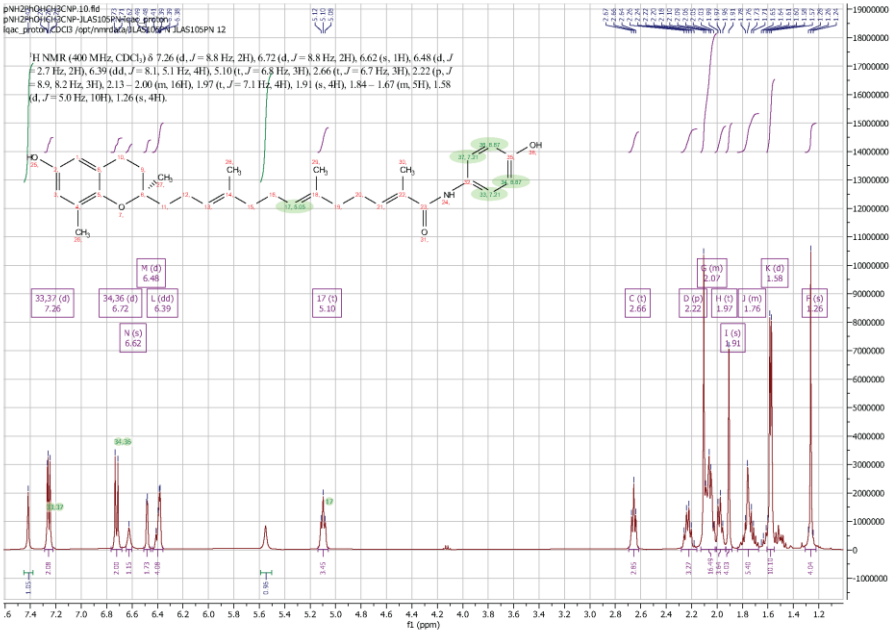

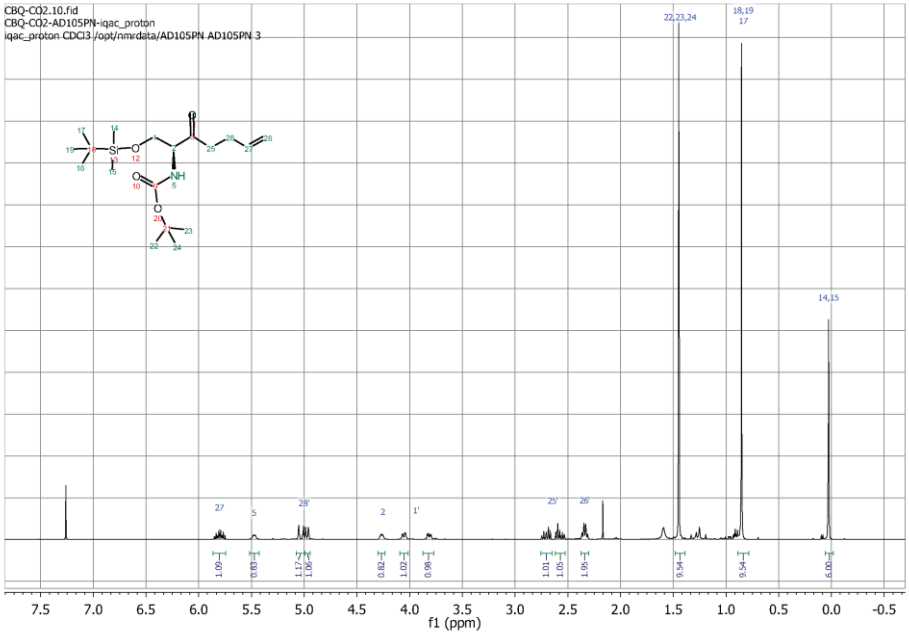
CBQ-CO2.10.fid
CBQ-CO2-AD105PN-iqac_proton
iqac_proton CDCl3 /opt/nmrdata/AD105PN AD105PN 3
22,23,24
18,19
17
14,15
27
5
28'
2
1'
25'
26'
1.09
0.83
1.17
1.06
0.82
1.02
0.98
1.01
1.05
1.95
9.54
9.54
6.00
7.5 7.0 6.5 6.0 5.5 5.0 4.5 4.0 3.5 3.0 2.5 2.0 1.5 1.0 0.5 0.0 -0.5
f1 (ppm)

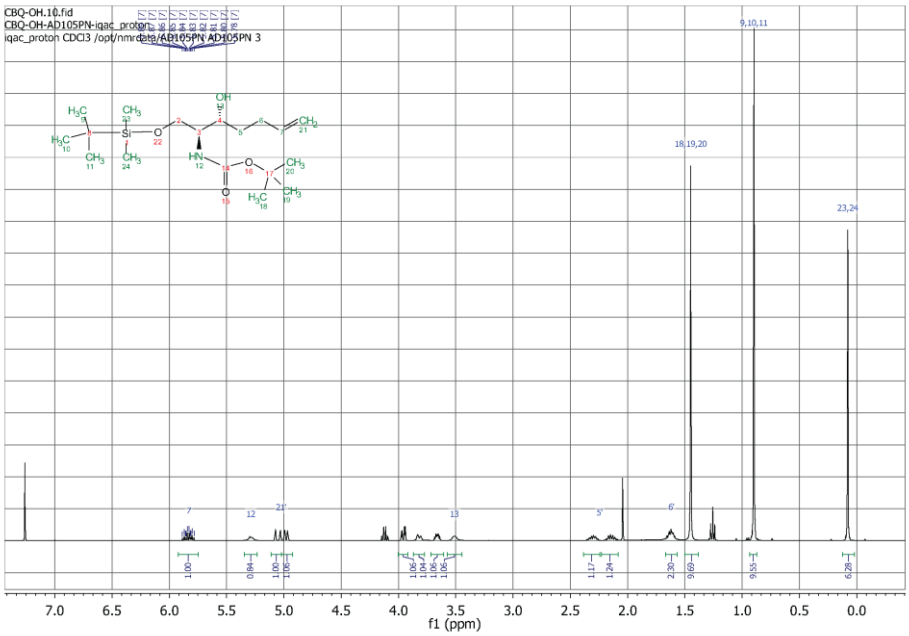
CBQ-OH.10.fid
CBQ-OH-AD105PN-iqac_proton
iqac_proton CDCl3 /opt/nmrdata/AD105PN AD105PN 3
9,10,11
18,19,20
23,24
7
12
21'
13
5'
6'
1.00
0.94
1.00
1.06
1.06
1.04
1.06
1.06
1.17
1.24
2.30
9.69
9.55
6.28
7.0 6.5 6.0 5.5 5.0 4.5 4.0 3.5 3.0 2.5 2.0 1.5 1.0 0.5 0.0
f1 (ppm)

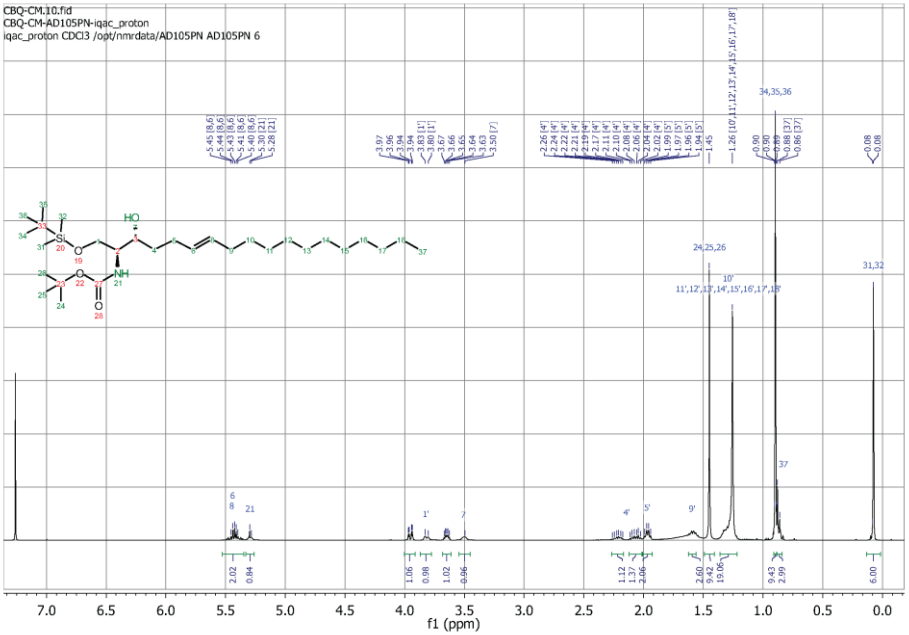
CBQ-CM-10.fid
CBQ-CM-AD105PN-iqac_proton
iqac_proton CDCl3 /opt/nmrdata/AD105PN AD105PN 6
f1 (ppm)

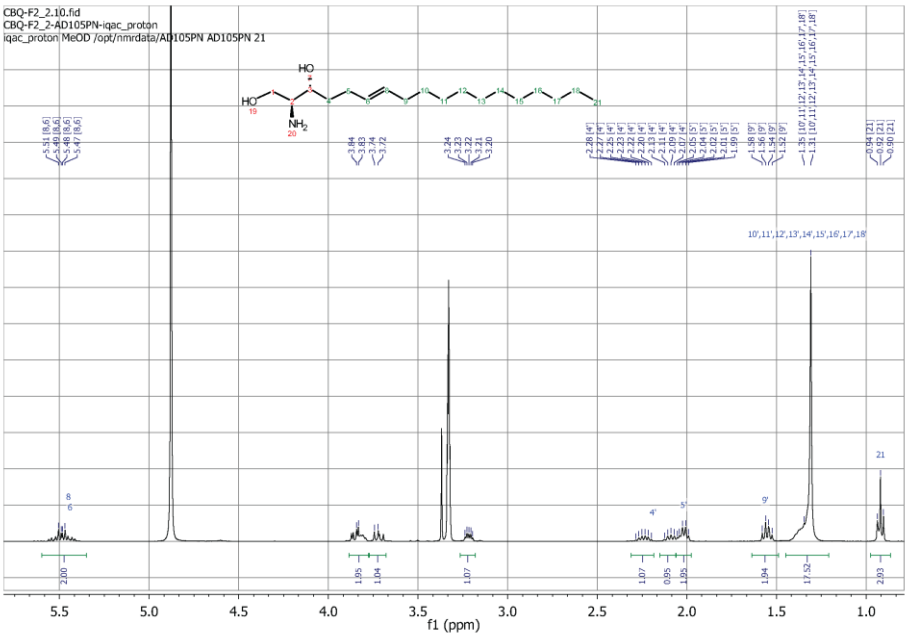
CBQ-F2_2-10.fid
CBQ-F2_2-AD105PN-iqac_proton
iqac_proton MeOD /opt/nmrdata/AD105PN AD105PN 21
f1 (ppm)

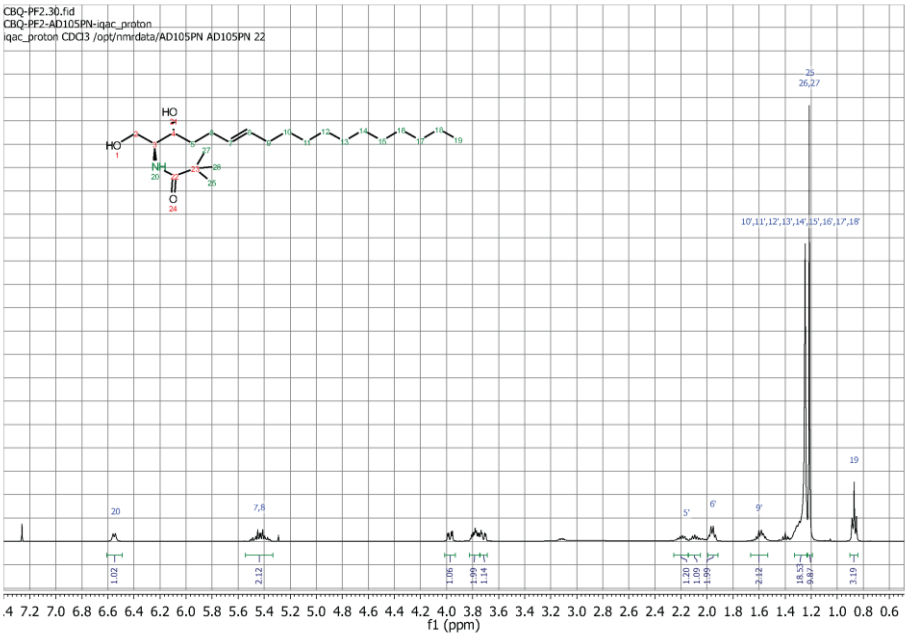
CBQ-PF2.30.fid
CBQ-PF2-AD105PN-iqac_proton
iqac_proton CDCl3 /opt/nmrdata/AD105PN AD105PN 22
HO
HO
NH
O
O
25
26,27
10',11',12',13',14',15',16',17',18'
19
20
7,8
5'
6'
9'
1.02
2.12
1.06
1.99
1.14
1.20
1.00
1.99
2.12
16.53
9.87
3.19
f1 (ppm)